Trapped to free: A mechanism to spatiotemporal chaos

Kaifen He
CCAST (World Laboratory), Box 8730, 100080 Beijing, China
and Institute of Low Energy Nuclear Physics, Beijing Normal University, 100875 Beijing, China
(Received 30 November 1998)

We further investigate the crisis-induced transition from temporal chaos (TC) to spatiotemporal chaos (STC) due to collision between the unstable orbit of a carrier saddle steady wave (SSW) and the attractor of its perturbation wave (PW) [Kaifen He, Phys. Rev. Lett. **80**, 696 (1998)]. In the present work, the influence of the SSW on its PW is studied in different dimensions. It is found that in our case, as a result of mode-mode couplings only one dimension becomes crucial in the onset of crisis. The state transition of the PW mode phase in this dimension at the crisis is emphasized. Before the crisis, all the PW partial waves are trapped in the SSW state. After the crisis, the PW partial wave in this dimension is free from the trapping of the SSW partial wave; it experiences on-off resonance with the latter, which is responsible for the transition to STC.
[S1063-651X(99)06605-2]

PACS number(s): 05.45.−a, 41.20.Jb, 47.27.−i, 52.35.−g

I. INTRODUCTION

A mechanism for the onset of turbulence has attracted much attention in recent years [2–4]. As pointed out in Ref. [5], the question of what is the actual mechanism of transition from laminar to turbulent motion is the most natural one we should try to answer, and when discussing turbulence one should speak of space-time chaos. Both time-chaos (TC state) and space-time chaos (STC state) are erratic in their time evolutions, so the essential difference between them is manifested in their spatial behaviors. How and why a TC state transits to a STC state is an interesting problem; its answer would be significant for our understanding of the onset of turbulence. In previous work [1], for a nonlinear wave system we found that the motion can display a sharp transition from a TC to a STC state, and a crisis [6–9] is responsible for the transition. The mechanism for the onset of the crisis in Ref. [1] can be summarized by the following points. A necessary condition for its occurrence is the existence of a saddle steady wave solution (a saddle point). If the saddle wave is perturbed, for the linear perturbation one can find stable and unstable orbits. When taking into account nonlinearity of the perturbation, its modes can build up a gap solitary wave which is trapped by the saddle steady wave. The motion of the gap solitary wave can bifurcate into a chaotic attractor. If the chaotic attractor collides with the saddle point, crisis occurs, which leads to very turbulent motion in contrast to the more laminarlike one before the crisis.

In the present work we study the mechanism further. Since a partial differential system such as that considered in Ref. [1] has infinitely many dimensions, it would be significant to know whether all the dimensions are important in the onset of the crisis, or if only one or a few dimensions play a crucial role. When analyzing the problem, a wave solution is divided into a saddle steady wave (SSW) and a perturbation wave (PW), as we did before. The PW is scattered at the carrier SSW; its motion is influenced by the latter as well as by its own nonlinearity. In the present work, such influences will be studied in respective dimensions. The paper is organized as follows. Section II is the formalism and relevant phenomena of the transition from TC to STC. In Sec. III we discuss the linear motion of PW under the influence of carrier SSW; the role of PW mode phases in the evolution of mode amplitudes is stressed. In the subsequent sections the nonlinearity of PW is taken into account. In Sec. IV we briefly introduce the mechanism for the onset of the crisis reported in Ref. [1]. In Sec. V we demonstrate that indeed one dimension may play a crucial role in the onset of the crisis. By further investigating the transition of the mode phase in the crisis, we conclude that it is the on-off resonance between the PW and SSW partial waves in this dimension that is responsible for the turbulent motion in the STC state. Finally, Sec. VI contains the discussion.

II. TRANSITION FROM TC TO STC STATE

The following driven/damped nonlinear drift-wave equation is used as our model:

$$\frac{\partial \phi}{\partial t} + a\frac{\partial^3 \phi}{\partial t \partial x^2} + c\frac{\partial \phi}{\partial x} + f\phi\frac{\partial \phi}{\partial x} = -\gamma\phi - \epsilon \sin(x - \Omega t), \tag{1}$$

where the 2π boundary condition is applied and $a = -0.287$, $c = 1.0$, $f = -6.0$, and $\gamma = 0.1$ are fixed throughout the paper. $\{\Omega, \epsilon\}$ are two control parameters. We focus on its steady wave solutions of saddle type (SSW) $\phi_0^*(x - \Omega t)$. Here the subscript 0 denotes steady wave and the asterisk superscript denotes saddle type. The wave energy of the system is $E(t) = (1/2\pi)\int_0^{2\pi}\frac{1}{2}[\phi^2 - a(\partial\phi/\partial t)^2]dx$.

As reported in Ref. [1], we find that solutions of Eq. (1) may display a transition from a TC to a STC state. Here the terminology ''transition'' has two meanings. First, for given Ω there exists a critical point $\epsilon = \epsilon_c$ for the transition; before and after the point the asymptotic states of the system are dynamically different. For instance, if we set $\Omega = 0.65$, the critical point is $\epsilon_c \simeq 0.20$. When $\epsilon = 0.19$, asymptotically the solution of Eq. (1) is of TC type, but when $\epsilon = 0.20$ or larger the asymptotic state is of STC type. Second, beyond the

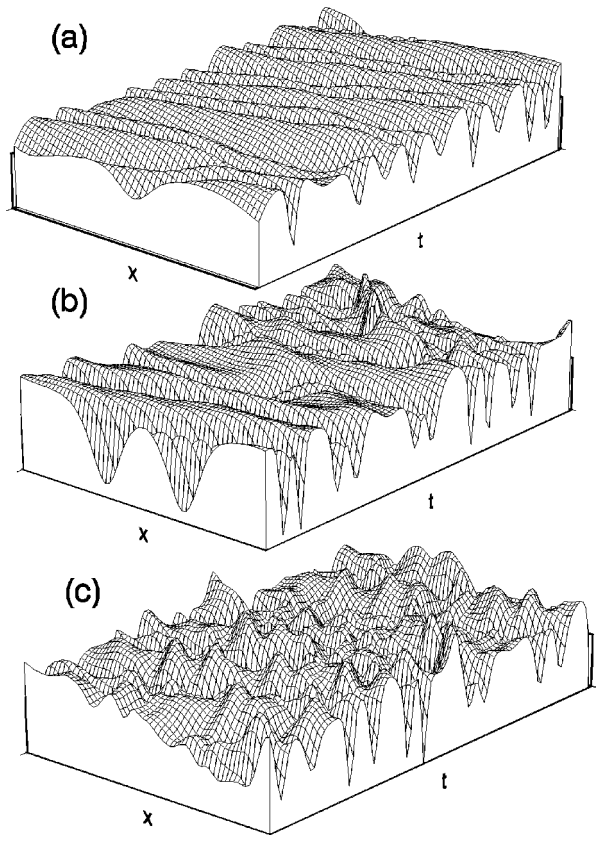

FIG. 1. Space-time patterns of $\phi(x,t)$ for (a) TC state, (b) around the critical transition time, (c) STC state for $\Omega=0.65,\epsilon=0.22$.

critical point, $\epsilon>\epsilon_c$, with fixed (Ω,ϵ) the time evolution of the system can show a sharp transition from a TC to a STC state.

As an example, Fig. 1 presents a sequence of space-time patterns displaying such a transition for $\Omega=0.65,\epsilon=0.22$. The results are obtained by solving Eq. (1) with a pseudospectral method. First, the motion is displayed as a laminarlike TC state, as Fig. 1(a) shows. Its time evolution is chaotic, but spatially it is regular. While it is a transient period in the time evolution (if the initial condition is properly chosen), the motion may stay in this TC state for a rather long time before it suddenly transits to a STC state. Figure 1(b) exhibits the space-time pattern just around the critical transition time. One can see very clearly how a laminarlike pattern is destroyed, which finally leads to a STC state. Figure 1(c) is the asymptotic pattern of the motion, very turbulent. It is a STC state, chaotic in time and erratic in space.

Here we did not present the example of the asymptotic TC state for $\epsilon\leqslant\epsilon_c$ (e.g., $\epsilon=0.19$), for its pattern is roughly the same as that of Fig. 1(a).

The TC and STC states as given in Fig. 1 show qualitatively different spatial behaviors. Figure 2 gives the time averages of wave-number spectra, $\langle\phi^2(k)\rangle=1/M[\Sigma_{i=1}^{M}\phi^2(k,t_i)]$, for (a) TC state, (b) STC state, which are the same as in Fig. 1. Here $\phi(k)$ is the spatial Fourier transform of $\phi(x)$. As can be seen from Fig. 2(a), for a TC state the spectral strength decreases exponentially, $\langle\phi^2(k)\rangle\sim e^{-\alpha k}$ with $\alpha=1.56\approx 3/2$, while in Fig. 2(b), for a STC state, the spectrum follows a power law, $\langle\phi^2(k)\rangle\sim k^{-\beta}$, here $\beta=2.43\approx 5/2$.

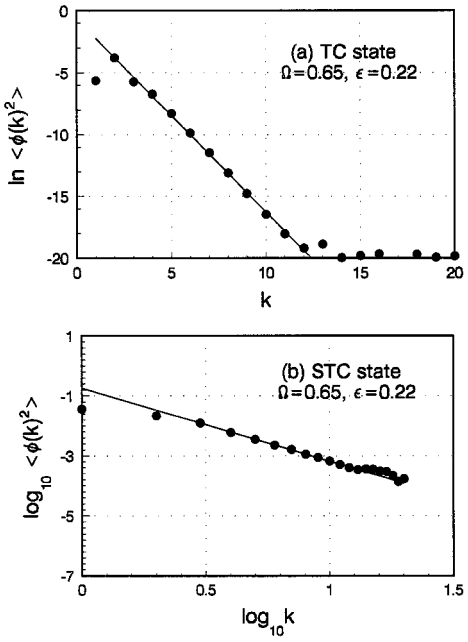

FIG. 2. Averaged spatial spectra, $\langle\phi^2(k)\rangle$, of (a) TC state, (b) STC state for the same case as Fig. 1, $\Omega=0.65,\epsilon=0.22$.

In order to test the above results, we have used two different methods. One is to solve Eq. (1) by a pseudospectral method, the other is to solve two sets of mode equations derived from Eq. (1) which we will describe in the following. To obtain Fig. 1 we used the former method, but in Ref. [1] the space-time patterns are obtained by the latter one. The two methods give qualitatively the same results. In particular, the laws followed by the wave-number spectra from the two methods are in good agreement with each other, respectively, for TC and STC states. This fact convinces us that the analysis for the mechanism in the following sections, which is based on the two sets of equations, is valid.

When transformed to $\xi=x-\Omega t,\tau=t$, a steady wave $\phi_0(\xi)$ satisfies the steady equation $\partial\phi_0(\xi)/\partial\tau=0$. By expanding $\phi_0(\xi)=\Sigma_{k=1}^{\infty}\phi_{0,k}(\xi)\equiv\Sigma_{k=1}^{\infty}A_k\cos(k\xi+\theta_k)$ we get a set of coupled algebraic equations from the steady equation,

$$
\begin{aligned}
&-k[c-(1-ak^2)\Omega]A_k\sin\theta_k+\gamma A_k\cos\theta_k\\
&-\frac{kf}{4}\Bigg(\sum_{i+j=k}A_iA_j\sin(\theta_i+\theta_j)+\sum_{i-j=k}A_iA_j\sin(\theta_i-\theta_j)\\
&\qquad+\sum_{j-i=k}A_iA_j\sin(\theta_j-\theta_i)\Bigg)=0,\\
&-k[c-(1-ak^2)\Omega]A_k\cos\theta_k-\gamma A_k\sin\theta_k+\epsilon\delta_{1,k}\\
&-\frac{kf}{4}\Bigg(\sum_{i+j=k}A_iA_j\cos(\theta_i+\theta_j)+\sum_{i-j=k}A_iA_j\cos(\theta_i-\theta_j)\\
&\qquad+\sum_{j-i=k}A_iA_j\cos(\theta_j-\theta_i)\Bigg)=0.
\end{aligned}
\tag{2}
$$

Here and in Eqs. (4), $k=1,2,\ldots,N\to\infty$. For given (Ω,ϵ), Eqs. (2) can be solved to give the solution $\phi_0(\xi)$.

Setting $\phi(\xi,\tau)=\phi_0(\xi)+\delta\phi(\xi,\tau)$, one obtains the following equation for $\delta\phi$ from Eq. (1):

$$\frac{\partial}{\partial\tau}\left(1+a\frac{\partial^2}{\partial\xi^2}\right)\delta\phi-\Omega\frac{\partial}{\partial\xi}\left(1+a\frac{\partial^2}{\partial\xi^2}\right)\delta\phi+c\frac{\partial\delta\phi}{\partial\xi}+\gamma\delta\phi+f\frac{\partial}{\partial\xi}[\phi_0(\xi)\delta\phi]+f\delta\phi\frac{\partial\delta\phi}{\partial\xi}=0. \tag{3}$$

Expanding $\delta\phi$ into Fourier modes, $\delta\phi(\xi,\tau)=\Sigma_{k=1}^{\infty}\delta\phi_k(\xi,\tau)\equiv\Sigma_{k=1}^{\infty}b_k(\tau)\exp i[k\xi+\alpha_k(\tau)]+\text{c.c.}$, one can calculate $\delta\phi(\xi,\tau)$ by solving the following set of ordinary differential equations:

$$\begin{aligned}\frac{db_k}{d\tau}=&-\frac{\gamma}{1-ak^2}b_k+\frac{fk}{2(1-ak^2)}\\&\times\Bigg\{\sum_{i+j=k}[A_ib_j\sin(\theta_i+\alpha_j-\alpha_k)+b_ib_j\sin(\alpha_i+\alpha_j-\alpha_k)]\\&+\sum_{i-j=k}[A_ib_j\sin(\theta_i-\alpha_j-\alpha_k)+b_ib_j\sin(\alpha_i-\alpha_j-\alpha_k)]\\&+\sum_{j-i=k}[A_ib_j\sin(-\theta_i+\alpha_j-\alpha_k)+b_ib_j\sin(\alpha_j-\alpha_i-\alpha_k)]\Bigg\},\end{aligned} \tag{4}$$

$$\begin{aligned}\frac{d\alpha_k}{d\tau}=&-k\left(\frac{c}{1-ak^2}-\Omega\right)-\frac{fk}{2(1-ak^2)b_k}\\&\times\Bigg\{\sum_{i+j=k}[A_ib_j\cos(\theta_i+\alpha_j-\alpha_k)+b_ib_j\cos(\alpha_i+\alpha_j-\alpha_k)]\\&+\sum_{i-j=k}[A_ib_j\cos(\theta_i-\alpha_j-\alpha_k)+b_ib_j\cos(\alpha_i-\alpha_j-\alpha_k)]\\&+\sum_{j-i=k}[A_ib_j\cos(-\theta_i+\alpha_j-\alpha_k)+b_ib_j\cos(\alpha_j-\alpha_i-\alpha_k)]\Bigg\}.\end{aligned}$$

Equations (2) and (4) are the two sets of equations we used to analyze the mechanism for the transition from TC to STC. In this treatment, no approximation is made. As mentioned above, the results from these equations (with appropriate truncation N) are qualitatively the same as those obtained by solving Eq. (1) with a pseudospectral method.

Generally speaking, as can be seen from Eqs. (3), except for the linear dispersion, the motion of $\delta\phi$ is influenced by two effects arising from the system nonlinearity: being scattered at the carrier wave, $\phi_0(\xi)$, and the nonlinearity of $\delta\phi$. In particular, if the steady wave is of saddle type (SSW), $\phi_0^*(\xi)$, the two effects cooperate in such a special way that they may cause a crisis-induced transition from TC to STC. As a first step, in the next section we discuss the linear response of PW $\delta\phi$ when scattered at the SSW $\phi_0^*(\xi)$, from which one can see the important role played by the mode phases of $\delta\phi$.

III. PHASE-LOCKING STABLE/UNSTABLE ORBITS OF LINEAR PERTURBATION MODES AT SSW

Now we calculate the linear orbit of PW scattered at a SSW. One way to show that a SW is of saddle type is to calculate the eigenvalues of PW modes. In general all the eigenvalues are complex conjugates. If one pair of eigenvalues is real, one positive, and one negative, saddle-node bifurcation occurs [10]; we refer to the steady wave as SSW. Obviously in this case there is only one unstable direction. However, this unstable direction projects onto every dimension in the phase space. In the present section, we calculate the stable and unstable orbits (SO and UO) of PW in respective dimensions by solving Eqs. (2) and Eqs. (4) in a linear approximation with respect to $\delta\phi(\xi)$ [i.e., we neglect the nonlinear term(s) of $\delta\phi$ or of $\{b_k\}$; in this section, when mentioning Eqs. (4) we always mean their linear approximations]. Here we should point out that, as can be seen from Eqs. (4), even the nonlinear terms of $\{b_k\}$ are neglected and the modes $\{b_k,\alpha_k\}$ are still coupled with each other through the modes of ϕ_0, $\{A_k,\theta_k\}$.

We start from a chosen SW at $\Omega=0.65,\epsilon=0.22$; from eigenvalue analysis we already know that it is a saddle type, $\phi_0^*(\xi)$. From Eqs. (4) with tiny initial $\delta\phi(\xi)$ we calculate the linear evolution of $\delta\phi$ scattered at carrier $\phi_0^*(\xi)$. As is well known, a saddle point has SO as well as UO. In the case of UO, the amplitudes b_k increase exponentially with time as expected; however a remarkable result is that the mode phases α_k approach a set of constants $\{\alpha_k^U\}$. This phenomenon can be seen in Fig. 3(a), which gives the temporal evolutions of $\alpha_k(\tau)$ at SSW $\phi_0^*(\xi)$ for $k=1-3$; one can see that the phases α_k quickly adjust to their respective constants. On the other hand, when reversing the time variable, one can follow the SO's backward to infinite amplitudes. Surprisingly, in this case the phases α_k also approach a set of constants $\{\alpha_k^S\}$, which is different from $\{\alpha_k^U\}$. This can be seen in Fig. 3(b), where the phases α_k start from the resulting values of Fig. 3(a); with time going to negative infinity they evolve to another set of constants. Notice that in every dimension k there are two UO's, but along both of them the mode phases α_k evolve asymptotically to the same set of constants. Similarly, in every dimension there are two SO's, along which the phases α_k approach another set of constant values.

From these results one can see that when scattered at SSW the linear PW mode phases have two stagnation points, $\{\alpha_k^S\}$ and $\{\alpha_k^U\}$. The orbit can be either stabilized or destabilized depending on which point the mode phases are attracted to. Since the phases of the carrier wave $\phi_0^*(\xi)$, θ_k's, are constants, the relative phases $(\alpha_k^{S,U}-\theta_k)$ are also invariable in every dimension. In fact, it is the phase difference

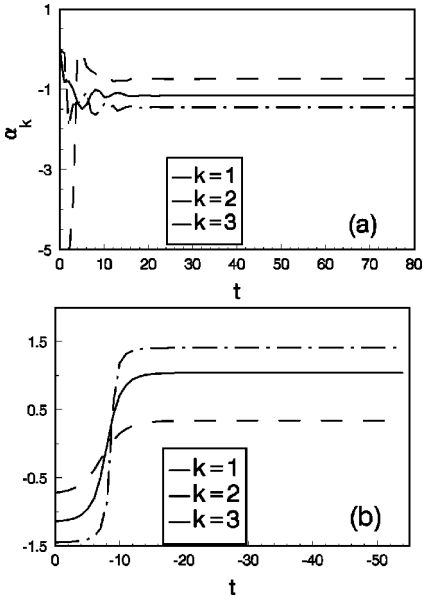

FIG. 3. (a) Time evolution (unstable orbit) and (b) reversed time evolution (stable orbit) of $\alpha_k(\tau)$ when PW is linearly scattered at carrier $\phi_0^*(\xi)$ with $\Omega=0.65, \epsilon=0.22,\ k=1-3$.

$(\alpha_k-\theta_k)$ that plays an important role in driving or damping the PW mode amplitude. Physically speaking, since PW is scattered by carrier SSW, its mode amplitudes are driven up by the carrier if all the relative phases take the ''favorable values,'' say, $\{\alpha_k^U-\theta_k\}$; in contrast, if they take the ''unfavorable values,'' $\{\alpha_k^S-\theta_k\}$, the mode amplitudes are damped by it. This phase-difference-related driving/damping effect causes the linear UO/SO of the saddle wave. When the nonlinearity of $\delta\phi$ is included, PW mode phases still play an important role. This fact can be seen in Sec. V. Before addressing this point, for the sake of comparison let us briefly introduce in the next section the crisis that causes the transition of TC to STC.

IV. CRISIS DUE TO COLLISION TO THE SADDLE POINT

In this and the following sections we calculate Eqs. (2) and the full Eqs. (4), that is, taking into account the nonlinear term with respect to $\delta\phi$ in Eqs. (3) [and Eqs. (4)]. In this case, the evolution of $\delta\phi(\xi,\tau)$ displays a crisis of heteroclinic tangency with the saddle point, leading to the transition from a TC to a STC state. Let us describe this phenomenon with a series of solutions in $\{\Omega,\epsilon\}$ parameter space.

After taking into account the nonlinearity with respect to $\delta\phi$, the PW mode amplitudes no longer go to infinity; in certain cases the modes can build up a solitary wave, which can be called a gap solitary wave [11,12]. In this case, the PW energy

$$\delta E(\tau)=\sum_k \delta E_k=\sum_k (1-ak^2) \times[A_k b_k \cos(\theta_k-\alpha_k)/2+b_k^2/4] \qquad (5)$$

tends to a constant. Figure 4 shows such an example for $\Omega=0.56, \epsilon=0.07$. Figure 4(a) is the evolution of $\delta E(\tau)$; Fig. 4(b) is the asymptotic wave form of $\delta\phi(\xi)$ $(+)$ in which $\phi_0^*(\xi)$ $(\triangledown)$ is also drawn. One can see that the gap solitary wave $\delta\phi_g(\xi)$ is trapped in the potential well of $\phi_0^*(\xi)$.

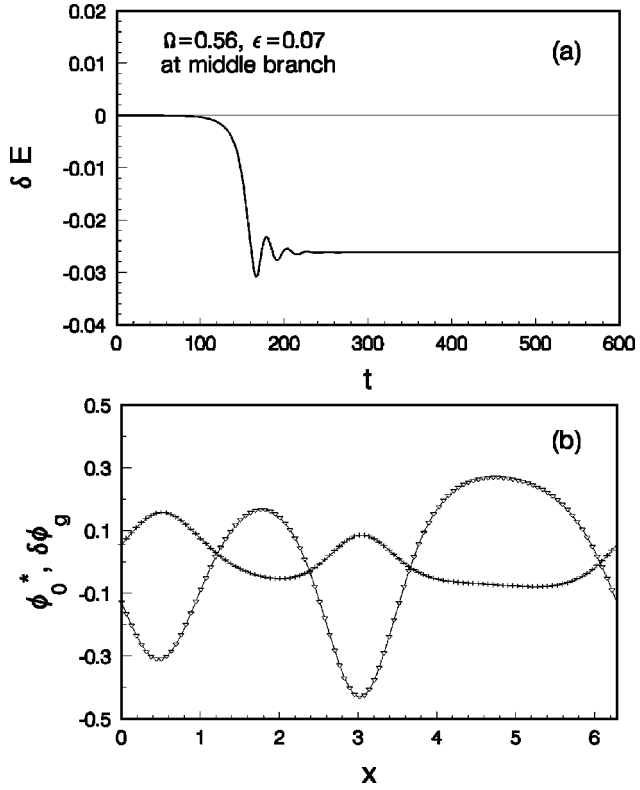

FIG. 4. A gap solitary wave built up by PW modes. (a) Time evolution of PW ''energy'' δE at SSW $\phi_0^*(\xi)$; (b) asymptotic gap solitary wave $\delta\phi_g(\xi)$ $(+)$ trapped in $\phi_0^*(\xi)$ $(\triangledown)$ for $\Omega=0.56, \epsilon=0.07$.

As the parameters are varied, the gap solitary wave loses stability. In Fig. 5, $\delta E_{k=2}(\tau)$ versus $\delta E_{k=1}(\tau)$ are plotted, where one can see how the crisis occurs due to heteroclinic

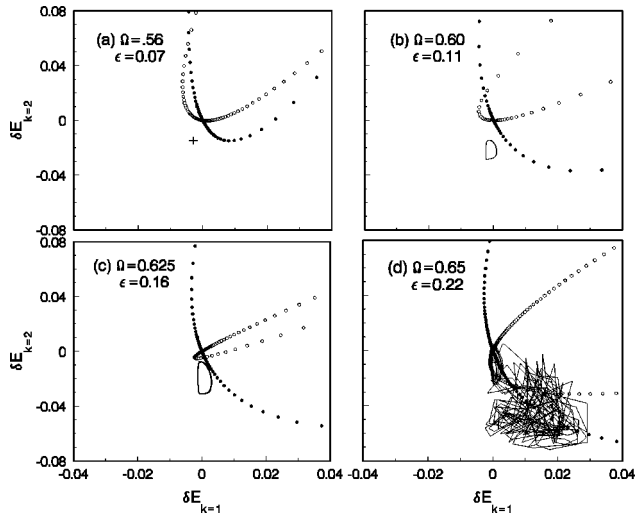

FIG. 5. Development of heteroclinic tangency in phase plot. $\delta E_{k=2}$ vs $\delta E_{k=1}$ with SSW $\phi_0^*(\xi)$ at (a) $\Omega=0.56, \epsilon=0.07$; (b) $\Omega=0.60, \epsilon=0.11$; (c) $\Omega=0.625, \epsilon=0.16$; (d) $\Omega=0.65, \epsilon=0.22$. The PW orbits are drawn by solid lines; bullets and circles denote the stable and unstable orbits of SSW.

tangency. In all the plots the carriers are chosen as saddle type. The bullets denote the linear SO's and the circles denote the linear UO's. In Fig. 5(a) [the same case as Fig. 4 for $\Omega=0.56,\epsilon=0.07$] the gap solitary wave is displayed as a fixed point (see ''+''). As the parameters are changed, the fixed point bifurcates to the limit cycle [Fig. 5(b) for $\Omega=0.60,\epsilon=0.11$]. The limit cycle gets larger and a little chaotic [Fig. 5(c) for $\Omega=0.625,\epsilon=0.16$]. Finally, in Fig. 5(d) the chaotic attractor collides with the linear unstable orbit of SSW (heteroclinic tangency), and the crisis occurs. One can see that at first the orbit travels in a small chaotic attractor for a while before suddenly jumping to a larger and much more chaotic one. When in the small attractor, the motion shows a TC state as in Fig. 1(a), while in the larger attractor the motion behaves as STC in Fig. 1(c).

V. STATE TRANSITION OF ONE PW MODE AND ON-OFF RESONANCE IN STC

The mechanism of the transition to STC has been shown to be a crisis of heteroclinic tangency. Now the question is what happens before/after the crisis at different dimensions. In this section we calculate the motion of a partial wave of PW in respective dimensions and study its relation to that of SSW, again by solving Eqs. (2) and the full Eqs. (4). We will demonstrate that one dimension plays a crucial role in the transition. For the present parameters, this dimension is $k=1$. Further, by studying the state transition of the PW mode phase in this dimension at the crisis, we show that on-off resonance between the PW and SSW partial waves is responsible for the turbulent motion after crisis.

In Fig. 6 we plot the $k=1$ partial wave of PW,

$$\delta\phi_k(\xi,\tau)=b_k(\tau)\cos[k\xi+\alpha_k(\tau)], \tag{6}$$

and that of SSW,

$$\phi^*_{0,k}(\xi)=A_k\cos(k\xi+\theta_k). \tag{7}$$

In the plots, triangles denote the SSW partial wave, $\phi^*_{0,k=1}(\xi)$, and bullets denote the PW partial waves at different times, $\delta\phi_{k=1}(\xi,\tau)$. (a) is before the crisis, (b) after the crisis. In the (ξ,τ) frame the carrier wave $\phi^*_{0,k=1}(\xi)$ is motionless. One can see very clearly that while the PW $\delta\phi_{k=1}(\xi,\tau)$ varies with time, its motion is strongly influenced by the existence of $\phi^*_{0,k=1}(\xi)$. In Fig. 6(a), before the crisis (TC state), the amplitudes of $\delta\phi_{k=1}(\xi,\tau)$ remain smaller than its carrier $\phi^*_{0,k=1}(\xi)$ and are trapped in the potential well provided by it. However, dramatic change occurs after the crisis (STC state). This can be seen in Fig. 6(b), in which the amplitude of $\delta\phi_{k=1}(\xi,\tau)$ can be much larger than that of $\phi^*_{0,k=1}(\xi)$. It is no longer trapped by the carrier partial wave. If we consider the PW partial wave as a ''particle,'' it seems now to become a ''free particle'' that can go over the barrier of the carrier wave, in contrast to before the crisis, when the ''particles'' are well confined by the potential.

Figure 7 shows the motion of a partial wave of $k=2$ as an example in dimensions other than $k=1$; again (a) is in a TC state and (b) in a STC state. In both cases the peaks of $\delta\phi_{k=2}(\xi,\tau)$ are well trapped in the valley of $\phi^*_{0,k=2}(\xi)$, and on average $\delta\phi_{k=2}(\xi,\tau)$ is antiphased with its carrier. The

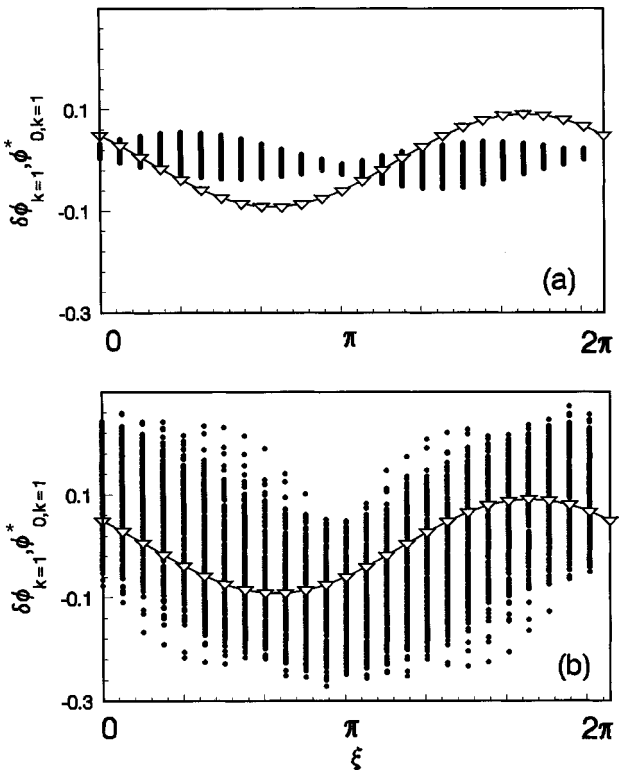

FIG. 6. Motion of partial wave $\delta\phi_{k=1}(\xi,\tau)$ (●) in partial wave $\phi^*_{0,k=1}(\xi)$ (▽) for (a) TC state, (b) STC state; the same case as in Figs. 1 and 2, $\Omega=0.65,\epsilon=0.22$.

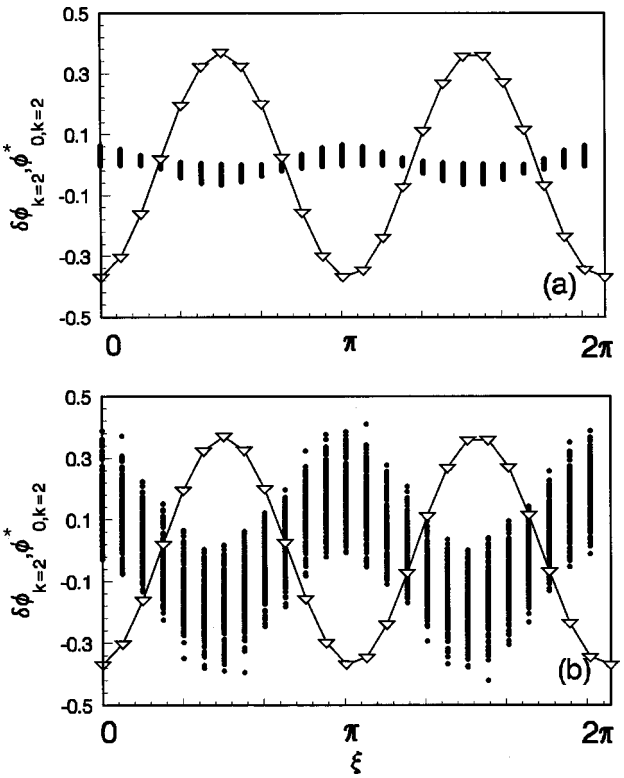

FIG. 7. Motions of partial waves $\delta\phi_{k=2}(\xi,\tau)$ (●) in partial wave $\phi^*_{0,k=2}(\xi)$ (▽) for (a) TC state, (b) STC state; the same case as in Figs. 1 and 2.

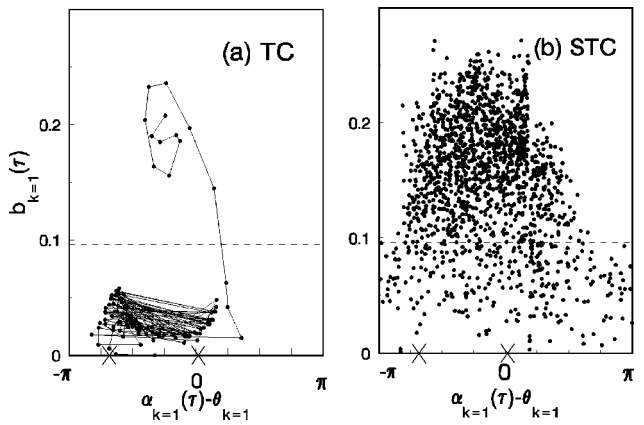

FIG. 8. $b_k(\tau)$ vs $\alpha_k(\tau)-\theta_k$ for $k=1$. (a) The same case as in Figs. 1(a) and 1(b), (b) the same case as in Fig. 1(c). The dashed line gives $A_{k=1}$. The two crosses on the abscissa indicate $\alpha_{k=1}^{S,U}-\theta_{k=1}$.

only difference between Figs. 7(a) and 7(b) is that in the latter case the amplitudes of $\delta\phi_{k=2}(\xi,\tau)$ can be comparable to that of carrier $\phi_{0,k=2}^{*}(\xi)$. The other high k modes have similar behavior.

In comparing Figs. 6 and 7 with Fig. 5(d) one can see that Figs. 6(a) and 7(a) correspond to the small attractor before crisis in Fig. 5(d), while Figs. 6(b) and 7(b) correspond to the larger and more chaotic one.

From the above results we realize that not all the dimensions are crucial for the dramatic change in the transition. In our case only $k=1$ is crucial for the qualitatively different dynamics after crisis. However, here we should stress that such a critical role of $k=1$ is a result of the cooperation of all the modes due to the system nonlinearity.

Now let us concentrate on the ''key dimension'' $k=1$. Recall in Sec. III in a linear approximation that we have shown that the phases of PW modes have a significant effect on their amplitude evolutions. Depending on the different phase-locking values, the orbits can be either stabilized or destabilized. When the nonlinearity of $\delta\phi$ is included, we would expect that the PW partial wave amplitudes should also be influenced by their phases or, more precisely, by the phase differences between the PW and SSW partial waves.

To clarify this problem, we study the PW amplitude $b_k(\tau)$ versus the phase difference $\alpha_k(\tau)-\theta_k$ between PW and SSW for $k=1$. The results are plotted by bullets in Fig. 8: (a) includes the results before the crisis and a few points at the critical moment of crisis (see the branch shooting up); (b) is after the crisis, in which mode $(-\pi,\pi)$ has been taken (so for clarity we did not connect the orbit points by lines). The dashed line gives the amplitude of the carrier partial wave, $A_{k=1}$. On the abscissa the two crosses indicate the stagnation phase points $\alpha_{k=1}^{S,U}$ (minus $\theta_{k=1}$) of the linear SO/UO, respectively (see Sec. III).

A remarkable difference can be seen when comparing Fig. 8(a) with Fig. 8(b). In the first place, in accordance with Fig. 6, in Fig. 8(a) before the crisis $b_{k=1}(\tau)$ remains smaller than the carrier amplitude $A_{k=1}$. Then at the critical moment when the crisis occurs, $b_{k=1}(\tau)$ suddenly increases and surpasses $A_{k=1}$. After the crisis in Fig. 8(b), $b_{k=1}(\tau)$ can be much larger than $A_{k=1}$. Furthermore, possibly more essential change occurs in the phase $\alpha_{k=1}(\tau)$ after crisis. In Fig. 8(a) the phase difference $\alpha_{k=1}(\tau)-\theta_{k=1}$ is confined within a regime, $\alpha_{k=1}^{U}\sim<\alpha_{k=1}(\tau)<\sim\alpha_{k=1}^{S}$. In the plot $\alpha_{k=1}(\tau)$ librates chaotically as that of a pendulum with chaotically varying length. In contrast, in Fig. 8(b) the variation of phase $\alpha_{k=1}(\tau)$ can go over 2π. In this case, while it librates chaotically, the ''pendulum'' also begins to whirl irregularly. To clarify the problem it is instructive to look at the equation for α_k in Eqs. (4). The motion of α_k is governed by two factors: the first term on the right-hand side of the equation causes linear rotation, and the other terms arise from a nonlinear effect. Those terms arising from the system nonlinearity also include two parts, one being contributions from the interaction between SSW and PW (SP terms) and the other from the self-nonlinearity of PW (PP terms). If b_k's are small, the motion of α_k is governed mainly by the first term, so it rotates. With the increase of b_k's, the nonlinear effect plays a more and more important role. In the case of a gap solitary wave as given in Fig. 4(b), an equilibrium is arrived at and the α_k's become constants. If the b_k's increase further, the nonlinear effect dominates and the fixed point of α_k loses stability, which leads to the TC state. However, in this case the SP terms still dominate the PP terms; the PW partial wave is nevertheless trapped by that of SSW. When the crisis occurs, the amplitude of one PW partial wave, $b_{k=1}(\tau)$, for the first time surpasses $A_{k=1}$ [see the vertically extending branch in Fig. 8(a)]; the PP terms can be comparable to or even stronger than the SP terms. In this case, $\alpha_{k=1}$ may once again become whirling. In our case, after the crisis the whirling belongs to the latter one dominated by PW self-nonlinearity. It is a complicated motion combining chaotic libration with rotation. We would like to refer to this as nonlinear whirling in order to distinguish it from the whirling that occurs in weak nonlinearity, e.g., in Ref. [13]. Consequently, the crisis essentially causes a transition of one PW mode phase, from a state of chaotic libration to a combination of chaotic libration and whirling.

It is realized that the PW motion is coupled with carrier SSW, so roughly speaking in the case of nonlinear whirling we have the following picture: the PW partial wave $\delta\phi_{k=1}(\xi,\tau)$ chaotically ''passes through'' the carrier partial wave $\phi_{0,k=1}(\xi)$ with the amplitude comparable to the latter. Therefore, the relative phase $\alpha_{k=1}(\tau)-\theta_{k=1}$ can take random values in the whole range $(-\pi,\pi)$. Since the amplitudes of two waves can compete with each other, it provides a possibility for them to become resonant. In Fig. 8(b) one can see that in a certain regime of phase difference (approximately between $\alpha_{k=1}^{U}$ and $\alpha_{k=1}^{S}$), the PW partial wave can be strongly increased. On average, its amplitude $b_{k=1}$ is larger than the carrier one $A_{k=1}$, while in the remaining regime the amplitudes are smaller than $A_{k=1}$. This phenomenon suggests that, as in the linear case of Sec. III, phase α_k or phase difference $\Delta_k=\alpha_k-\theta_k$ plays a significant role. In the favorable regime of $\Delta_{k=1}$, the amplitude $b_{k=1}$ is increased by the carrier partial wave. In this case, if in addition their amplitudes are comparable, the two waves, $\delta\phi_{k=1}(\xi,\tau)$ and $\phi_{0,k=1}^{*}(\xi)$, are approximately in resonance; on the other hand, in the unfavorable regime, $\delta\phi_{k=1}$ is damped by the latter, and they are not in resonance. As this process repeats again and again, the amplitude of $\delta\phi_{k=1}$ is pushed up and down randomly by the potential of the carrier partial wave.

This phenomenon indicates that a kind of on-off resonance occurs between the $k=1$ PW partial wave and the SSW partial wave, which is responsible for the spatiotemporal chaotic motions after the crisis.

On the other hand, the other modes $k=2,3,4,\ldots$ do not show such a dramatic difference before and after the crisis. Either before or after the crisis, the PW partial wave amplitudes remain smaller than those of the corresponding SSW modes.

When $\epsilon<\epsilon_c$, e.g., $\epsilon=0.19$, the motion of the $k=1$ partial wave is similar to Fig. 6(a), which will not be presented here.

VI. DISCUSSION

In the present work we further investigated the mechanism of crisis-induced transition to STC that is relevant to the existence of a saddle point in a nonlinear wave system solution. Linear stable and unstable orbits of SSW are shown to be phase-locked, respectively. When the full nonlinearity is considered, we find that the crisis also induces a state transition of one mode phase. Before the crisis, all the partial waves of PW are well trapped in that of the carrier SSW, respectively, while after the crisis one PW partial wave is free from the confinement of SSW; it experiences random on-off resonance with the latter. It is concluded that this on-off resonance is responsible for the turbulent behavior in the STC state.

In the parameter regime we are concerned with in the present work, one dimension turns out to be crucial in the onset of a crisis as a result of mode-mode couplings. However, it does not exclude the fact that with parameter variations other dimensions may also display qualitatively different behaviors, such as $k=1$, before and after crisis. If this happens, it would cause more and more complicated turbulent motions.

ACKNOWLEDGMENTS

This work was supported by the National Natural Foundation of China (Grant No. 19675006), Project of Basic Research of China ''Nonlinear Science,'' and partly supported by the Foundation for Doctoral Training of National Education Committee of China.

[1] Kaifen He, Phys. Rev. Lett. **80**, 696 (1998).
[2] M.C. Cross, P.C. Hohenberg, Rev. Mod. Phys. **65**, 851 (1993).
[3] H. Chate and P. Manneville, Phys. Rev. Lett. **58**, 112 (1987).
[4] H. Xi, X. Li, and J.D. Gunton, Phys. Rev. Lett. **78**, 1046 (1997).
[5] R.Z.Sagdeev *et al.*, *Nonlinear Physics From the Pendulum to Turbulence and Chaos* (Harwood Academic Publishers, London, 1988), Chap. 11, pp. 457–460.
[6] C. Grebogi, E. Ott, and J.A. Jorke, Phys. Rev. Lett. **48**, 1507 (1982); C. Grebogi, E. Ott, and F. Romerias, Phys. Rev. A **36**, 5365 (1987).
[7] H.B. Stewart, Y. Ueda, and C. Grebogi, Phys. Rev. Lett. **75**, 2478 (1995).
[8] J.C. Sommerer, E. Ott, and C. Grebogi, Phys. Rev. A **43**, 1754 (1991); J.C. Sommerer, W.L. Ditto, C. Grebogi, E. Ott, and M.L. Spano, Phys. Rev. Lett. **66**, 1947 (1991).
[9] E. Ott, *Chaos in Dynamic Systems* (Cambridge University Press, New York, 1993), p. 277.
[10] Kaifen He and Gang Hu, Phys. Lett. A **168**, 341 (1992).
[11] W. Chen and D.L. Mills, Phys. Rev. Lett. **58**, 160 (1987).
[12] Kaifen He and Luqun Zhou, Phys. Lett. A **231**, 65 (1997).
[13] S.H. Strogatz, Nature (London) **378**, 444 (1995).